Unmasking the J-wave: 3D ECG shows terminal depolarization mimicking early repolarization

Alejandro Jesús Bermejo Valdés[a,*]

[a] *Riojan Health Service, Logroño, Spain*

Abstract

Three-dimensional (3D) electrocardiography (ECG) was used to track the J-wave across viewing planes not accessible to standard two-dimensional (2D) ECG. This method revealed a J-loop structure expressed through three morphological and topological patterns, each indicating that the loop was embedded within different regions of the terminal QRS complex. This raises a conceptual issue: although the J-wave is empirically linked to phase-1 of the ventricular action potential, its 3D trajectory occupied regions typically associated with depolarization. These observations suggest that the conventional definition of the J-point position may require reconsideration within a 3D spatial framework.

Keywords: Three-dimensional ECG, J-wave, Early repolarization, 3D loops

*Corresponding author: ajbermejo@riojasalud.es

1. Introduction

The J-wave, classically defined as a positive deflection at the end of the QRS complex, appears in conditions such as early repolarization (ER), Brugada syndrome, hypercalcemia, or hypothermia, and has been associated with arrhythmogenic vulnerability and sudden cardiac death [1]. Experimental work has attributed its cellular and molecular basis to the I_{to} channels of cardiomyocytes from different myocardial layers, whose differential expression generates the phase-1 notch of the ventricular action potential [2, 3]. Despite this mechanistic insight, the diagnostic interpretation of the J-wave remains challenging because the terminal QRS complex and the onset of the ST segment constitute a transitional zone in which late depolarization and the initial phase of repolarization may coexist. This ambiguity underscores the need for a more precise electrophysiological interpretation.

In principle, the presence of a J-wave should be traceable across precordial leads, maintaining a coherent spatial position. It is physiologically inconsistent to observe a J-wave at the end of depolarization in one lead while the corresponding point appears embedded within the QRS complex in another lead. However, the conventional 12-lead electrocardiogram (ECG) provides only a restricted set of two-dimensional (2D) projections of cardiac electrical activity, thereby precluding continuous visualization of the spatial relationships between leads.

Our recent work has shown that standard leads can be used to reconstruct a continuous three-dimensional (3D) electrical loop that preserves the spatial relationships between leads [4]. This framework enables terminal deflections to be tracked across viewing planes [5], thus exposing projection-dependent

distortions that are invisible in conventional analysis. Here, using this 3D method, we evaluate how terminal QRS deflections migrate and transform across precordial orientations and identify distinct phenotypes of J-wave behavior.

2. Methods

Signals were obtained from the PTB Diagnostic ECG Database [6]. For each selected recording, we extracted the first complete cardiac cycle occurring within the initial 2000 ms of the trace, sampled at 1000 Hz. Signal preprocessing was performed in Python 3.13.3 using the `NumPy`, `WFDB`, and `Matplotlib` libraries. A 0.5 Hz high-pass Butterworth filter was applied to remove baseline drift, and a 40 Hz low-pass Butterworth filter was used to suppress high-frequency noise while preserving J-wave morphology. Signal quality and spectral content were verified to be consistent with conventional clinical filtering (50 Hz notch; 0.05-150 Hz bandwidth).

3D ECG reconstruction followed our previously described approach [4, 5]. For each case, the precordial signals were mapped into a 3D space using the coordinates `(V1, V6, time)`. The 3D loops were rendered using `Matplotlib`'s `mplot3d` engine, and the segment corresponding to the J-wave was highlighted in red.

We selected patients with a J-wave in V5 or V6. Recordings with excessive noise or strictly filiform 3D loops, which prevent reliable geometric tracking [5], were excluded. The final dataset consisted of 26 patients.

All figures, code, and patient-specific time windows are provided in the associated Mendeley Data repository [7].

3. Results

Three J-loop phenotypes emerged from 3D tracking of the terminal QRS deflection across precordial orientations.

3.1. Group i: Concealed J-loop unmasked by 3D rotation

In these recordings, the 3D J-loop corresponding to the 2D J-wave is concealed in the V1 projection and becomes visible only after rotating the 3D ECG, meaning that it is undetectable on standard 2D ECG (Fig. 1).

This group included 21 cases (80.8 %): 017/s0053lre, 040/s0219lre, 045/s0147lre, 048/s0171lre, 049/s0173lre, 052/s0190lre, 083/s0268lre, 165/s0322lre, 173/s0305lre, 180/s0374lre, 198/s0402lre, 241/s0469_re, 245/s0474_re, 248/s0481_re, 249/s0484_re, 250/s0485_re, 252/s0487_re, 258/s0494_re, 259/s0495_re, 273/s0511_re, and 277/s0527_re.

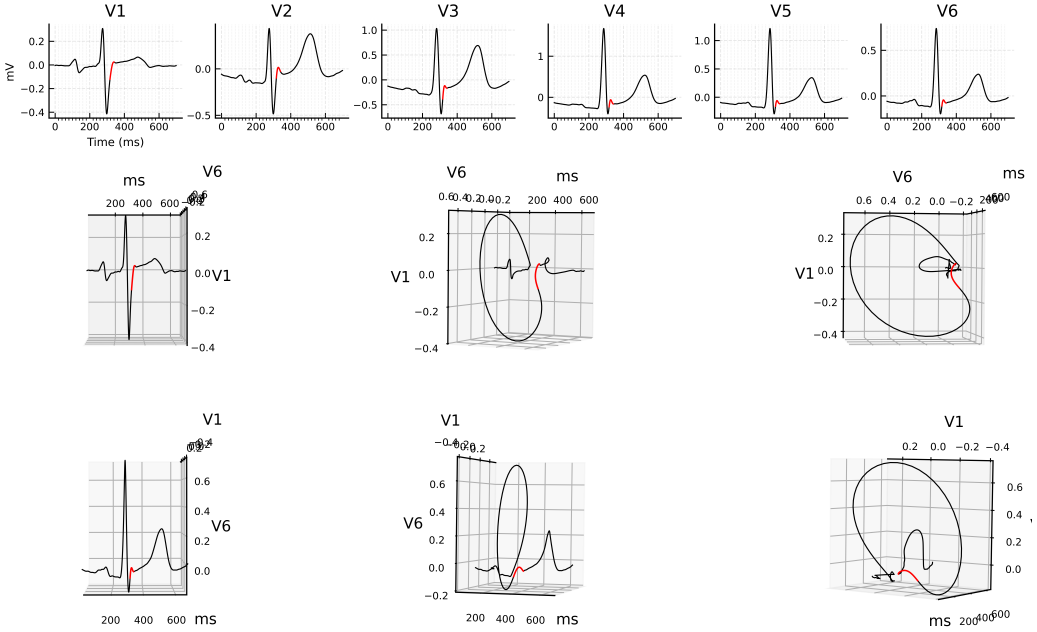

Figure 1: Group *i*: Representative example (patient 180). Top row: precordial leads V1-V6. Middle and bottom rows: 3D ECG loops displayed from different viewing orientations. The deflection corresponding to the J-wave is concealed in the V1 projection and becomes identifiable only when the 3D loop is rotated. The J-wave region is highlighted in red.

3.2. Group ii: J-loop polarity symmetry

In this phenotype, the J-wave in V6 remains spatially linked to a small terminal QRS deflection in V1 with the same polarity, irrespective of the V1-V6 3D rotation (Fig. 2). We refer to this behavior as polarity symmetry of the J-loop under rotational viewing. This group includes the following cases (11.5 %): 043/s0141lre, 230/s0454_re, and 244/s0473_re.

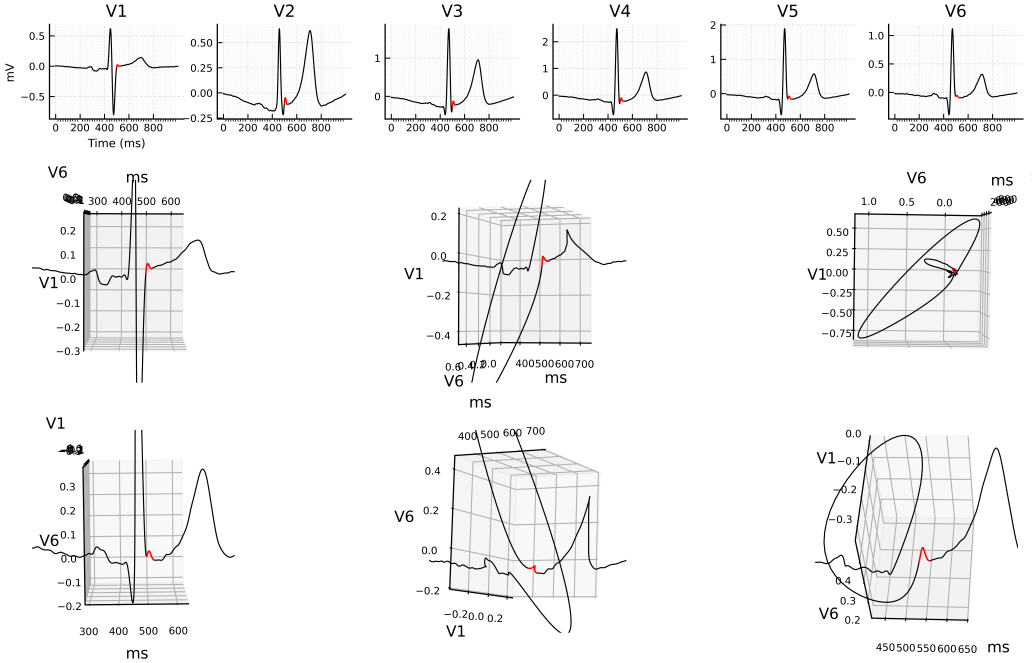

Figure 2: Group *ii*: Representative example (patient 244). Top row: precordial leads V1-V6. Middle and bottom rows: 3D ECG loops viewed from different orientations. The J-wave region (highlighted in red) preserves its positive polarity from V1 through the V6-oriented projections. A slight zoom was applied to the 3D views to enhance visualization.

3.3. Group iii: J-loop polarity inversion

In this group (Fig. 3), the configuration resembles that of group *ii* but with polarity inversion: a small negative terminal deflection in V1 becomes a J-wave as the 3D rotation approaches the V6 orientation. The recordings that exhibited this behavior are (7.7 %): 150/s0287lre and 187/s0207_re.

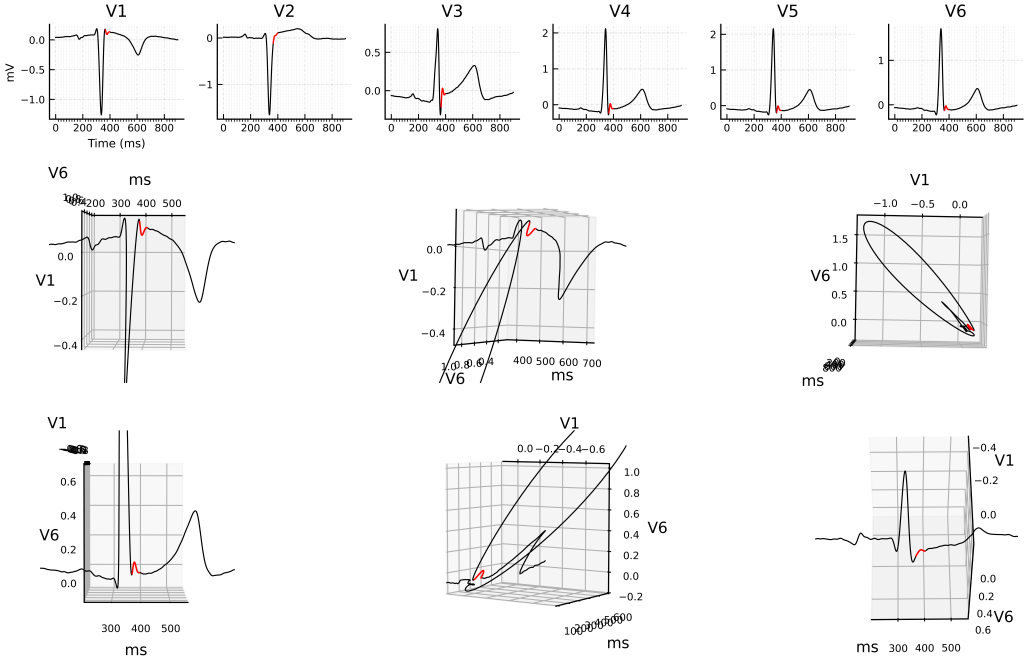

Figure 3: Group *iii*: Representative example (patient 150). Top row: precordial leads V1-V6. Middle and bottom rows: 3D ECG loops viewed from different orientations. As the viewing angle transitions from the V1- toward the V6-oriented projection, the J-wave region (highlighted in red) shifts from a small negative terminal deflection in V1 to a J-wave in V6. A slight zoom was applied to the 3D views to enhance visualization.

4. Discussion and Conclusions

Across the three phenotypes examined, we observed that the same underlying terminal J-deflection can adopt different morphologies depending on the viewing plane. In the first and most frequent group (≈ 81 %), the deflection corresponding to the J-position in V6 is embedded within the terminal QRS in V1. Only the 3D reconstruction reveals its continuity, which manifests as a J-loop concealed behind the V1 projection.

In the second group, a symmetric terminal J-loop preserves polarity throughout the V1-V6 rotation, producing a small J-wave. In the third group,

a polarity inversion emerges as the 3D loop is rotated, indicating that the presence or absence of inversion depends on the loop geometry within the terminal QRS region. Despite these morphological differences, the spatial positions of the J-wave in these two groups form a loop topology that lies near the classical J-point location, yet still falls within the terminal QRS region in the V1 projection.

Our observations, largely derived from group *i*, may refine the conventional understanding of the J-wave by showing that a deflection located at the J-position cannot be assumed to reflect the initial phases of repolarization unless its spatial coherence across leads is demonstrated. If the J-wave is interpreted as a manifestation of repolarization, then the terminal portion of the QRS in V1 must also be regarded as being influenced by repolarization. Conversely, if the terminal QRS in V1 represents a depolarization phenomenon, then its projection in V6 (manifesting as the J-wave) must likewise arise from depolarization. The planar ECG lacks the geometric information required to resolve this ambiguity, particularly regarding the continuity and morphology of J-loops. 3D tracking is therefore essential to determine whether a deflection and its associated loop seen at the onset of the ST segment in one lead occupies the same relative position in others, to assess how it becomes concealed or distorted by planar projections, and to establish its true 3D morphology.

Our results support three complementary interpretations of the J-wave:

4.1. The J-wave as an ER phenomenon

If the J-wave indeed marks the onset of repolarization in V6, the terminal portion of the QRS in V1 must be regarded as reflecting the same repolarization process, though it remains invisible on the planar tracing because

the corresponding J-loop is concealed within the 2D projection. This view is consistent with the classical mechanistic model in which the transient outward current I_{to} generates a phase-1 notch capable of producing ER patterns [1–3]. Under this interpretation, the J-wave should maintain a coherent temporal and spatial position across all precordial projections, an expectation rarely tested in 2D but directly verifiable using 3D ECG. This behavior may also explain the slurring often seen embedded within the terminal QRS complex in patients with ER [1]. Interestingly, in patient 045 (Appendix A.1), the slurring on the descending limb of the V6 R-wave transformed into a J-wave following a slight temporal-axis rotation of the 3D loop, indicating that slurring and the J-wave may represent the same underlying phenomenon viewed from different 3D projections of the ECG.

The presence of a J-wave or QRS slurring is a necessary, although not sufficient, criterion for the ER pattern, which additionally requires a J-peak amplitude of at least 0.1 mV in $\geq$2 contiguous leads (excluding V1-V3) and a QRS duration <120 ms [1]. However, our analysis indicates that the amplitude, morphology, and even the apparent presence of the J-wave depend on the projection plane of a higher-dimensional ECG representation and can be tracked throughout the entire 3D ECG space.

4.2. The J-wave as the terminal portion of ventricular depolarization

Our data also support an alternative mechanism, opposite to the former, in which the J-wave arises from terminal depolarization rather than from the initial phase of repolarization. This model is compatible with clinical observations describing J-wave appearance in diseases with conduction delay such as non-compaction cardiomyopathy, arrhythmogenic right ventricular

cardiomyopathy, and myocardial ischemia [8].

4.3. The J-wave as a transition zone where depolarization and repolarization coexist

A third possibility is that the J-wave reflects a transitional zone in which late phase-0 of the action potential coexists with phase-1, as a result of temporal dispersion in depolarization and repolarization across different myocardial regions. Anatomical spacing and cellular heterogeneity across myocardial layers may allow repolarization to begin in one region while depolarization continues in another, both contributing to the same surface deflection. The coexistence of these processes within the terminal QRS may explain why slurring in ER often merges seamlessly with the end of depolarization.

Across these three conceptual frameworks, the overarching implication is that the surface J-wave should not be regarded as a fixed electrophysiological entity but rather as the visible projection of a 3D electrical process whose interpretation depends on geometric context. In this perspective, 3D ECG emerges not only as a tool for visualizing J-loops and their morphology but also as a potential approach for clarifying the geometric origin of the J-wave, a hypothesis that will require confirmation through future experimental and clinical studies.

Appendix A. Slurring-to-J-wave transition

Appendix A.1. Recording 045

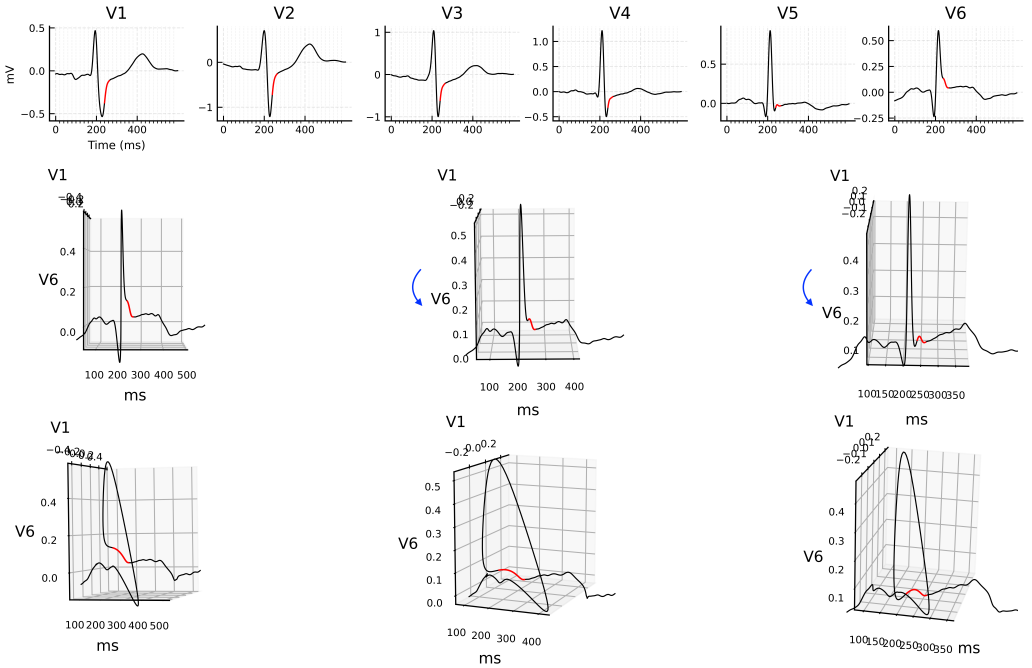

Figure A.4: 3D reconstruction of recording 045/s0147lre showing the slurring-to-J-wave transition. Top row: V1-V6 leads. Middle row: 3D ECG in the V6-oriented view. Bottom row: the same 3D loop after a slight leftward rotation. Curved blue arrows indicate the rotation direction. The J-wave is highlighted in red.

References

[1] J-wave syndromes expert consensus conference report: Emerging concepts and gaps in knowledge, Heart Rhythm 13 (10) (2016) e295–e324, focus Issue: Sudden Death. doi:10.1016/j.hrthm.2016.05.024.

[2] C. Antzelevitch, G.-X. Yan, J wave syndromes, Heart Rhythm 7 (4) (2010) 549–558, epub 2009 Dec 11. doi:10.1016/j.hrthm.2009.12.006.

[3] C. Antzelevitch, J. M. Di Diego, J wave syndromes: What's new?, Trends in Cardiovascular Medicine 32 (6) (2022) 350–363. doi:10.1016/j.tcm.2021.07.001.

[4] A. J. Bermejo Valdés, Three-dimensional standard electrocardiogram: A first approach based on precordial leads, Journal of Electrocardiology 89 (2025) 153875, epub 2025 Jan 20. PMID: 39892036. doi:10.1016/j.jelectrocard.2025.153875.

[5] A. J. Bermejo Valdés, R-wave progression or r-wave rotation? a 3d ecg-based perspective, Journal of Electrocardiology 91 (2025) 154047, epub 2025 Jun 7. PMID: 40513181. doi:10.1016/j.jelectrocard.2025.154047.

[6] R. Bousseljot, D. Kreiseler, A. Schnabel, Nutzung der ekg-signaldatenbank cardiodat der ptb über das internet, Biomedizinische Technik 40 (Suppl 1) (1995) 317.
URL https://physionet.org/content/ptbdb/1.0.0/

[7] A. J. Bermejo Valdés, 3d ecg: J-wave groups dataset (2025). doi:10.17632/myhw9rcjp3.1.

[8] A. S. Tsvetkova, J. E. Azarov, O. G. Bernikova, A. O. Ovechkin, M. A. Vaykshnorayte, M. M. Demidova, P. G. Platonov, Contribution of depolarization and repolarization changes to j-wave generation and ventricular fibrillation in ischemia, Frontiers in Physiology Volume 11 - 2020 (2020). doi:10.3389/fphys.2020.568021.